Bioconjugate Chemistry

pubs.acs.org/bc

Communication

A Self-Assembling Probe for Imaging the States of Golgi Apparatus in Live Single Cells

Weiyi Tan, Qiuxin Zhang, Pengyu Hong,* and Bing Xu*

Cite This: https://doi.org/10.1021/acs.bioconjchem.2c00084

Read Online

ACCESS | Metrics & More | Article Recommendations | Supporting Information

ABSTRACT: Despite the enormous progress in genomics and proteomics, it is still challenging to assess the states of organelles in living cells with high spatiotemporal resolution. Based on our recent finding of enzyme-instructed self-assembly of a thiophosphopeptide that targets the Golgi Apparatus (GA) instantly, we use the thiophosphopeptide, which is enzymatically responsive and redox active, as an integrative probe for revealing the state of the GA of live cells at the single cell level. By imaging the probe in the GA of live cells over time, our results show that the accumulation of the probe at the GA depends on cell types. By comparison to a conventional Golgi probe, this self-assembling probe accumulates at the GA much faster and are sensitive to the expression of alkaline phosphatases. In addition, subtle changes of the fluorophore results in slightly different GA responses. This work illustrates a novel class of active molecular probes that combine enzyme-instructed self-assembly and redox reaction for high-resolution imaging of the states of subcellular organelles over a large area and extended times.

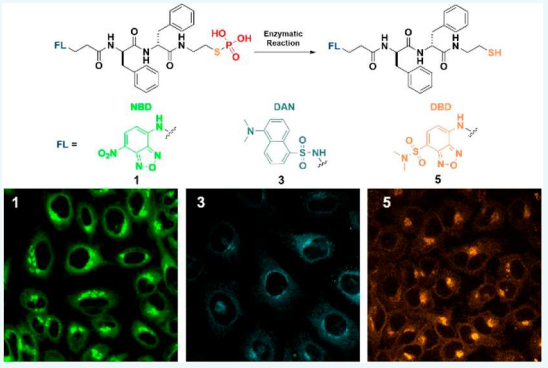

This communication reports an enzymatically responsive and redox active probe for revealing the state of the Golgi Apparatus (GA) at the single cell level. Genomics and proteomics have made extraordinary progress in oncology. However, exclusively relying on proteogenomics remains insufficient for diagnosis and treatment because of the complexity and dynamics of cancer. There are urgent needs to develop innovative approaches that integrate other forms of molecular data (e.g., molecular imaging) with proteogenomics to further our understanding of cancer and improve patient care.[1] An important direction toward this goal is to assess the dynamics of live cells in real time via molecular imaging. While considerable work has focused on developing a specific molecular probe for one desired target,[2−6] it is less common to use one probe to report the dynamics of multiple cellular processes in the context of subcellular organelles.[7] We serendipitously found a thiophosphopeptide (**1**), which is a substrate of alkaline phosphatase (ALP) and is redox active, for selectively targeting the GA.[8] GA, acting as the intracellular transportation portal[9,10] and dynamically regulating multiple cellular processes during cell cycles in mammalian cells, is considered a hub for different signaling pathways that drive the survival and migration of cancer cells.[11−13] Thus, we reckon that the state of the GA of cancer cells may provide a potential indicator of the dynamics of cancer subcellular organelles.

Toward to the development of the self-assembling probe for revealing the state of the GA of cancer cells, we need to test the probe in different cell lines, as well as compare the performance of the probes with existing ones. Here we report that the thiophosphopeptide acts as a self-assembling, single-cell GA probe for imaging the enzymatic and redox dynamic of the GA. The green fluorescence merges well with the red fluorescence after treating Golgi-RFP HeLa cells with **1** (10 μM), confirming the accumulation of the probe at the GA (Figure S1). As shown in Figure 1, the thiophosphopeptide, above its critical micelle concentration, mainly enter cells via caveola-mediated endocytosis.[8] Being dephosphorylated at the GA,[8] the resulting thiopeptide (**2**) undergoes three types of actions—self-assembling, forming covalent dimers, and attaching to cysteine rich proteins (CRPs)—for its building up at the GA. By imaging the probe in the Golgi of live cells, our results show that the accumulation of the probe depends on the type of cells. The rate of the accumulation of the probes in the GA largely correlates with the expression level of ALP and the intracellular level of the ROS/GSH (redox feature) of the cells. Moreover, by comparison to a conventional GA probe, C6-NBD-ceramide, this integrative probe images the Golgi state much faster and is more sensitive. In addition, we found that changing the different fluorophores results in slightly different GA secretion, suggesting that tuning the structures of the

Special Issue: What Comes after Liposomes? Self-Assembled Systems

Received: February 14, 2022
Revised: March 11, 2022

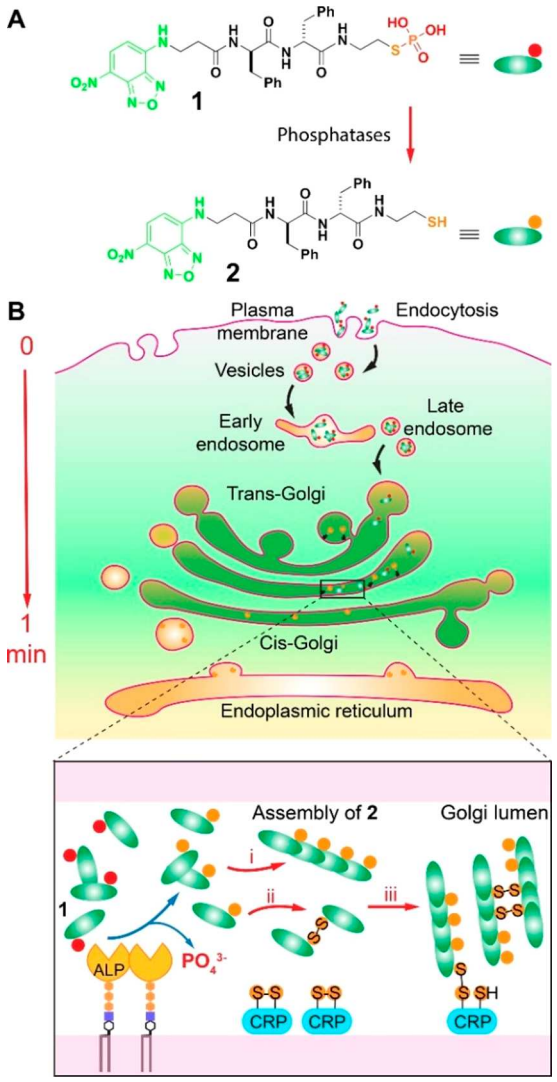

Figure 1. (A) Structure of the thiophosphopeptide (**1**) and the corresponding thiopeptide (**2**). (B) Transformation of **1** and **2** at the Golgi apparatus: (i) self-assembly, (ii) formation of covalent dimers, and (iii) attaching to cysteine rich proteins.

fluorophores may help reveal different processes involved by the GA. This work illustrates a novel class of active molecular probes that combine enzyme-instructed self-assembly and redox reaction for high-resolution imaging over a large area and extended time at the single cell level.

Figure 1A shows the structure of the thiophosphopeptide (**1**), having D-diphenylalanine as the backbone and 4-nitro-2,1,3-benzoxadiazole (NBD) and cysteamine *S*-phosphate[14] as the N-terminal and C-terminal caps, respectively. D-Diphenylalanine acts as the motif to enable self-assembly,[15] NBD exhibits enhanced fluorescence in the hydrophobic environment of supramolecular assemblies formed after enzymatic dephosphorylation,[16] the thiophosphate group serves as a substrate of ALP for enzyme-instructed self-assembly,[17,18] and the resulting thiopeptide is able to form a disulfide bond with cysteine rich proteins (CRPs). We used solid-phase peptide synthesis (SPPS) to synthesize **1** according to a previous report.[8] We observed a morphological change of **1** from nanoparticles to nanosheets after the addition of ALP *in vitro* (Figure S2), verifying that **1** undergoes self-assembly after the enzymatic reactions. As shown in Figure 1B, our previous studies[8] have revealed that **1** has the critical micelle concentration (CMC) of about 6.0 μM. The use of mβCD for slowing down the accumulation of **1** (Figure S3) suggests that **1** enters the cells by caveolin-mediated endocytosis when **1** is incubated with cells at 10 μM. After being generated by enzymatic dephosphorylation, **2** self-assembles to give bright fluorescent at the GA. Because of the oxidative environment at the GA, **2** also forms dimers (Figure S4) and likely links with cysteine rich proteins (CRPs) via the formation of disulfide bonds.[8] We also observed the morphological differences of the GA (i.e., Golgi fragmentation) between each individual cell (Figure S5), which supports the assumption of heterogeneous GA states. These results suggest that it is feasible to use **1** as an integrative probe to reveal the state of GA at the single cell level because the fluorescent intensity correlates with multiple cellular processes related to GA, such as endocytosis,[19] enzymatic dephosphorylation,[20] and redox mediated[21] formation of disulfide bonds.

We evaluated the accumulation of **2** at GA of each cell when incubating cells with **1** at concentrations of 5, 2, and 1 μM, and 500 nM. We used a confocal microscopy to take a video of fluorescent imaging at the GA of the HeLa cells incubated with **1**; then, according to the position of the nuclei and the fluorescence at the GA, we wrote an imaging analysis code to generate the curve that reflect the fluorescence at the GA of each cell versus the time of incubation (Figure 2A). At 5 μM of **1**, the fluorescence at the GA of all the HeLa cells is nonzero at 1 min (Figure S6), confirming the ability of **1** for almost instantly targeting and imaging the GA. However, the fluorescence at the GA is near zero when the concentration of **1** is 2 μM, 1 μM, and 500 nM (Figure S6). These results not only confirm that the fluorescence at the GA depends on the concentrations of **1** but also provides a threshold concentration of **1** for instantly imaging the state of the GA of the HeLa cells.

To determine how the concentration of **1** contributes to GA imaging, we compare the time needed for the GA of the HeLa cells to exhibit significant fluorescence at different incubating concentrations. Roughly, the time needed is proportional to the concentration of **1**. It takes about 30 min for significant fluorescence (e.g., a.u. = 0.1) at the GA of the HeLa cells incubated with 500 nM of **1**. When the incubation of **1** is 1 μM, 15 min of incubation is more than enough for significant fluorescence appearing at the GA. When the incubation of **1** is 2 μM, 7 min of incubation allows significant fluorescence to appear at the GA. When the incubation of **1** is 5 μM, 3 min of incubation is able to generate more fluorescence at the GA than those of the fluorescence at 7 min of the cells incubated by 2 μM of **1**. At each of the concentrations, the fluorescence increase differs for individual cells, reflecting that the state of the GA of individual cells also differs. Notably, the average GA fluorescent intensity at 3 min of the HeLa cells incubated with 5 μM of **1** is significantly higher than those at 30 min of the cells incubated with 500 nM of **1**, implying that the modes of endocytosis of **1** at 5 μM differ from those at 500 nM incubation concentrations. We used Methyl-β-Cyclodextrin (mβCD) and Cytochalasin D (CytD) as inhibitors for caveolin-mediated endocytosis and macropinocytosis, respectively, to examine the way of cellular uptake at different concentrations (Figure S7). The results indicate that **1** at 500 nM (much lower than its CMC) enters the HeLa cells predominantly by macropinocytosis, and **1** at 5 μM (nearly equals to its CMC) enters the HeLa cells by caveolin-mediated endocytosis as well as macropinocytosis.

https://doi.org/10.1021/acs.bioconjchem.2c00084
Bioconjugate Chem. XXXX, XXX, XXX−XXX

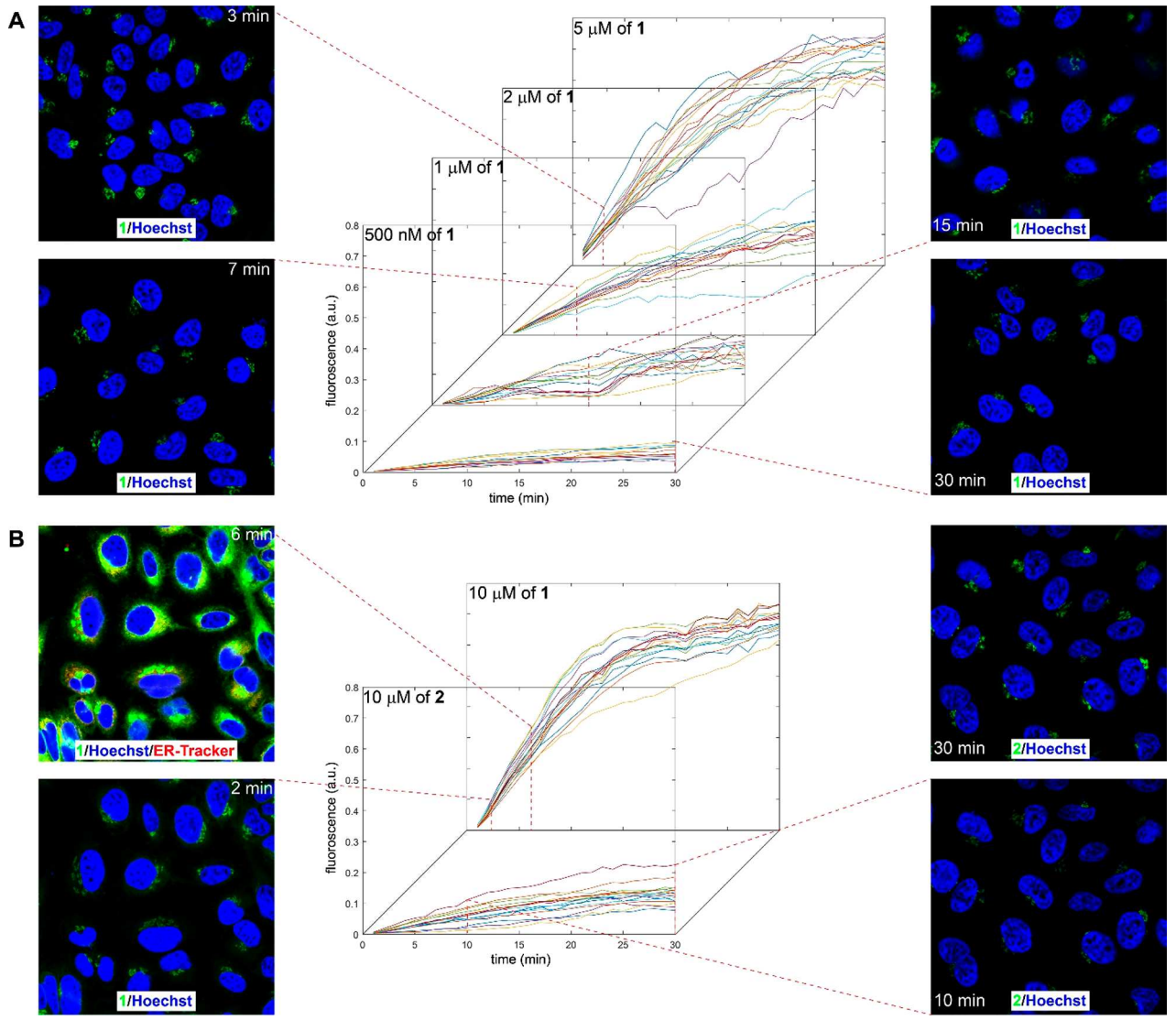

Figure 2. Single cell analysis of fluorescence intensity of the GA and CLSM images of HeLa cells treated with (A) **1** with different concentrations (5 μM, 2 μM, 1 μM, 500 nM) and (B) **1** and **2** (10 μM). Each curve indicates the temporal response of one cell.

To understand the role of dephosphorylation for imaging of the GA, we compared the fluorescence in the HeLa cell incubated with 10 μM of **1** to that in the HeLa cells incubated with 10 μM of **2**. The rate of increase of the fluorescence is much faster in the HeLa cells incubated by **1** than in the HeLa cells incubated by **2** (Figure 2B). At 2 min of incubation of **1**, the GA of the HeLa cells exhibits fluorescence comparable to that in the HeLa cells incubated by **2** at 10 min. At 30 min, HeLa cells incubated by **1** exhibit about 4 times higher fluorescence than HeLa cells incubated by **2**. At 6 min of HeLa cells incubated with 10 μM of **1**, some of the fluorescence has already started to overlap with the fluorescence of the ER-tracker, suggesting retrograde transport of the assemblies of **2** from the GA to the ER. On the other hand, at 30 min of the HeLa cells incubated by **2**, the fluorescence remains exclusively at the GA. This observation not only confirms the superior ability of **1** for imaging GA, but also indicates that the thiol group contributes to the localization of **2** at the GA. Moreover, replacing D-phenylalanine in **1** by D-alanine completely eliminates the ability of the thiophosphopeptide (**7**) to accumulate at the GA of HeLa cells (Figure S8), indicating that the self-assembling ability provided by D-diphenylalanine is critical for targeting the GA of cells.

We selected 10 μM of **1** to study the GA imaging on different cell lines because **1** enters HeLa cells swiftly at this concentration and is able to induce the cellular response in a short period of time. As shown in Figure 3A, fluorescence intensities increase rapidly at the GAs of Saos-2, HeLa, OVSAHO, SJSA-1, and HCC1937 cells, but the increase of the fluorescence is modest for HepG2, Capan-2, OVCAR4, PC-3, and B16F10. Notably, although the fluorescence build-up rates at the GA of HeLa and Saos-2 are similar, the fluorescence intensities at the GA of HeLa cells reach a plateau in less than 20 min, while the fluorescence intensities at the GA of Saos-2 cells continue to grow even at the 30 min time point, which agrees with the report of oligomeric ALP at the Golgi of HeLa cells.[22] The fluorescence intensities increase much more slowly at the GA of SKOV-3, VCap, HEK293, SH-SY5Y, H460, HS-5, MCF-7, and T98G cells (Figure 3B). These results indicate that a selective accumulation of the probe at the GA depends on cell types. Although this observation may be expected, how each type of cell accumulates the thiophosphopeptide probe at

https://doi.org/10.1021/acs.bioconjchem.2c00084
Bioconjugate Chem. XXXX, XXX, XXX−XXX

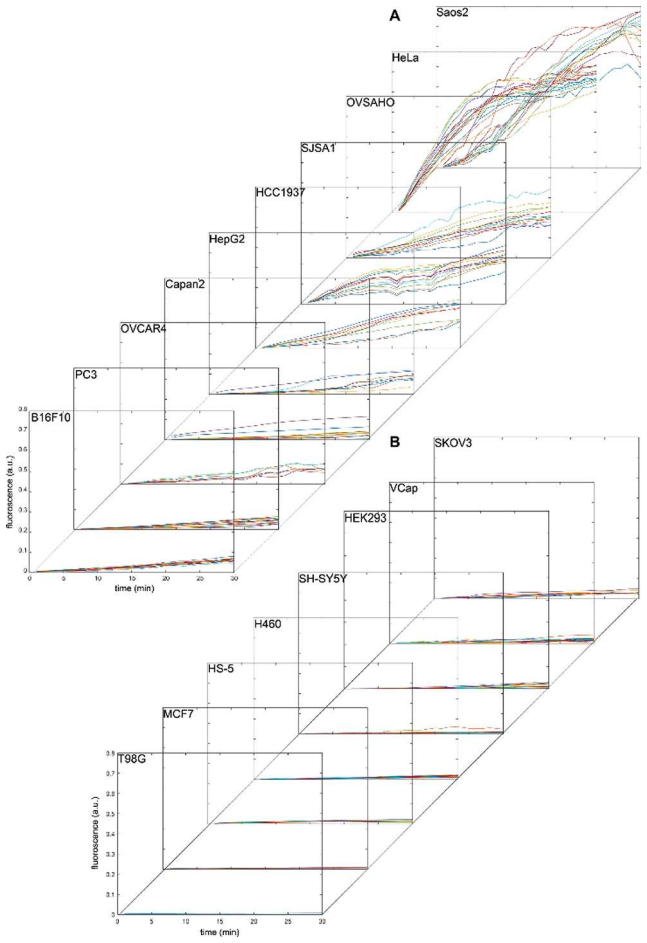

Figure 3. Single cell analysis of fluorescence intensity of the GA of different cell lines with (A) high or modest or (B) low intracellular fluorescence buildup treated with **1** (10 μM); each line represents the normalized fluorescence intensity at the GA of a single cell.

the GA is unknown. Moreover, this observation differs from the accumulation of C6-NBD-ceramide at the GA, which is almost the same level for the three cell lines. Thus, **1** would be a useful probe to reflect the dynamics in the GA. The rate of fluorescence build-up at the GA of different cell lines matches well with their expression level of ALP (Figure S9). HepG2, however, appears to be an outlier. That is, HepG2 shares a similar ALP expression level with OVSAHO,[23] but a much lower GA accumulation rate compared to that of OVSAHO. This exception partially originates from the high level of glutathione in hepatocytes[24] interfering with the accumulation of **2** at GA. To further verify the significance of the redox-active property to accumulate at the GA, we treated HepG2 cells with 2-methoxyestradiol (2-ME; 10 μM), an ROS inducer,[25] for 18 h to generate a more oxidative environment inside the cells. The pretreatment of HepG2 cells with 2-ME (an ROS inducer) results in a faster accumulation rate of **1** in the GA of the treated HepG2 cells than in HepG2 cells untreated with 2-ME (Figure S10). This result indicates that the oxidative environment contributes to the GA accumulation by favoring the dimerization of **2**.

To further assess the ability of **1** as a self-assembling and integrative probe, we compared it with the commercial Golgi probe, C6-NBD-ceramide,[26] using three representative cell lines: HeLa, HepG2, and HS-5. Comparing to HeLa and HepG2 cells, HS-5 has a low ALP expression. Although HepG2 cells overexpress ALP, there is a high intracellular concentration of glutathione (GSH), a reductant that interferes with the formation of disulfide bonds. As shown in Figure 4,

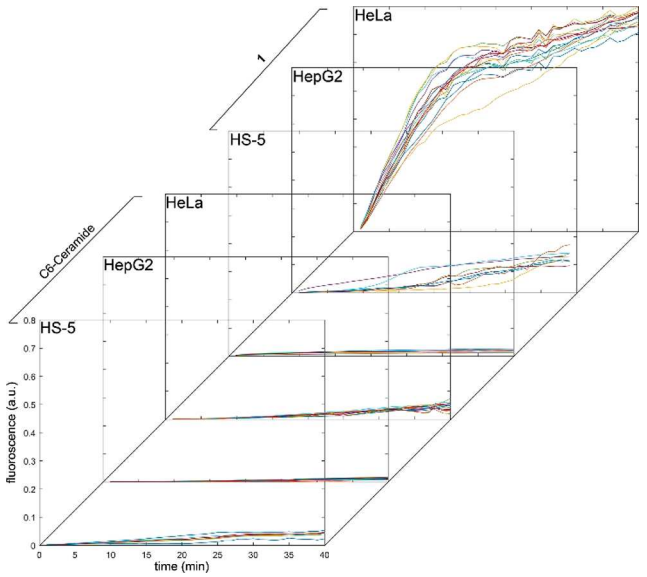

Figure 4. Single cell analysis of fluorescence intensity of the GA of HeLa, HepG2, and HS-5 treated with **1** (10 μM) or C6-NBD-ceramide (10 μM). Each line represents the normalized fluorescence intensity at the GA of a single cell.

the increase of fluorescence in the three cells follows the order of HeLa > HepG2 > HS-5 when the cells are incubated with **1**. However, when the cells are incubated with C6-NBD-ceramide, the increase of the GA fluorescence exhibits the trend of HeLa ≈ HS-5 > HepG2. At about 40 min of incubation, the GA fluorescence of HeLa cells obtained from incubation with C6-NBD-ceramide is less than one-tenth of that from incubation with **1**. On the other hand, the GA fluorescence of HS-5 cells obtained from incubation with C6-NBD-ceramide is higher than that from incubation with **1**. This result agrees with the following: (i) HS-5 hardly expresses ALP and (ii) the negative charge of **1** results in less uptake by HS-5 compared to the case of C6-NBD-ceramide. Notably, the GA fluorescence of HepG2 cells obtained from incubation with C6-NBD-ceramide is also lower than that from incubation with **1**, indicating that the enzymatic reaction plays a key role in the GA accumulation of **2**.

To generate GA-targeting thiophosphopeptides that emit at different excitation wavelengths, we replaced the NBD in **1** by 5-naphthalene-1-sulfonyl (DAN) or 4-(*N*,*N*-dimethylsulfamoyl)-2,1,3-benzoxadiazole (DBD) to synthesize **3** or **5** (Figure 5A). Both **3** and **5** enter HeLa cells quickly and accumulate at GA in less than 8 min (Figure 5B). Interestingly, there is a subtle difference in the location of the corresponding dephosphorylated products **4** and **6** after incubating the HeLa cells with **3** and **5** for 60 min (Figure 5B). Specifically, there are many tiny fluorescent puncta formed around the cells after about 10 min treatment of **3** on HeLa cells (Figure S11); they are spherical with various sizes, which are mainly located at the cytosolic area. In the case of **5**, there are few fluorescent puncta inside the HeLa cells; only larger spherical aggregates formed in culture media when HeLa cells were treated with **5** (Figure 5B). Considering that all three thiophosphopeptides have excellent GA targeting ability, the difference of the

https://doi.org/10.1021/acs.bioconjchem.2c00084
Bioconjugate Chem. XXXX, XXX, XXX−XXX

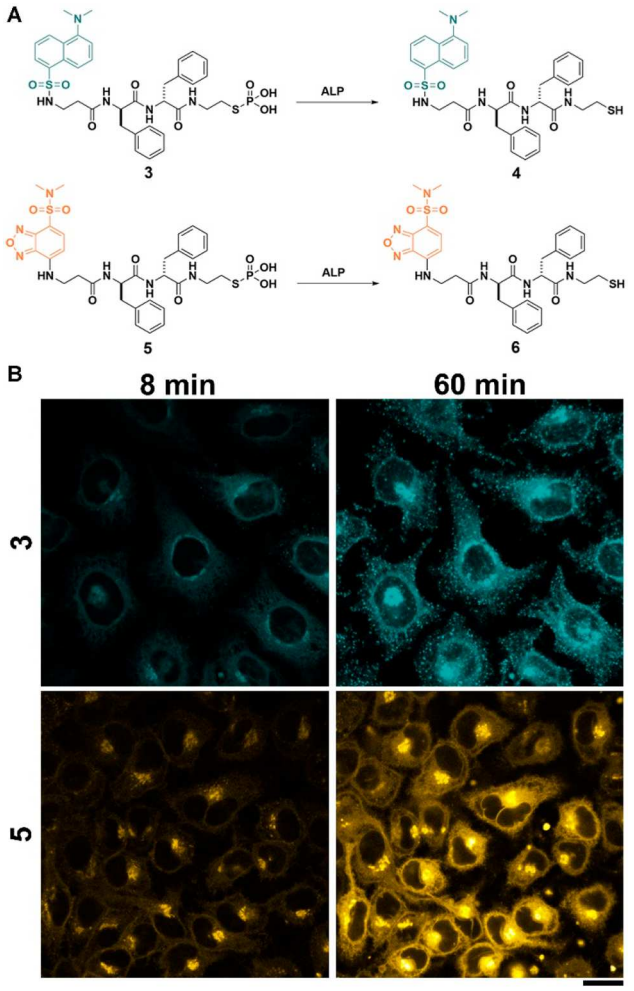

Figure 5. (A) Chemical structures of **3** and **5**, as well as their corresponding dephosphorylation products **4** and **6**, and (B) CLSM images of HeLa cells treated with **3** (10 μM) or **5** (10 μM) for 8 and 60 min. Scale bar = 20 μm.

subcellular location of the probes indicates that subtle structure differences of the fluorophores may bias them to slightly different secretory pathways that are mainly manipulated by GA.

In conclusion, this work reports a new type of self-assembling probes for understanding the functions of the GA at the single cell level. The increasing understanding of the protein trafficking to and from the Golgi[27] underscores the unique importance of GA for elucidating and modulating cell functions. Obviously, the state of the GA can be defined from different perspectives, such as genomic or proteomic. This work mainly refers to the dynamic accumulation of the probes made of phosphothiopeptides as one of the states of the GA. The self-assembling probes shown in this work may provide a useful tool to not only monitor the GA of different types of cells but also reveal heterogeneity in the same cell lines. Although numerous phosphatases exist inside cells, ALP is an almost perfect enzyme,[28] which has high catalytical efficiency. Thus, the dephosphorylation and accumulation of the thiophosphopeptides would reflect the expression of ALP and its activities related to the GA. Although this work uses ALP to activate the probes, the molecular architecture should be applicable to other enzymes for combining the enzyme-instructed self-assembly with redox reactions for the GA targeting and monitoring the state of the GA and further indicate the dynamics of cancer cells. Future studies will be on the influence of fluorophores for Golgi secretion, since it is known that different fluorophores affect cell uptake differently.[29] The concept demonstrated in this work may also lead to the combination of self-assembly with other intracellular reactions or subcellular interactions for revealing the potential communications between organelles.

■ ASSOCIATED CONTENT

Supporting Information

The Supporting Information is available free of charge at https://pubs.acs.org/doi/10.1021/acs.bioconjchem.2c00084.

Materials and detailed experimental procedures, mass spectra, and CLSM images (PDF)

■ AUTHOR INFORMATION

Corresponding Authors

Bing Xu − *Department of Chemistry, Brandeis University, Waltham, Massachusetts 02454, United States;* orcid.org/0000-0002-4639-387X; Email: bxu@brandeis.edu

Pengyu Hong − *Department of Computer Science, Brandeis University, Waltham, Massachusetts 02453, United States;* Email: hongpeng@brandeis.edu

Authors

Weiyi Tan − *Department of Chemistry, Brandeis University, Waltham, Massachusetts 02454, United States;* orcid.org/0000-0001-5316-8278

Qiuxin Zhang − *Department of Chemistry, Brandeis University, Waltham, Massachusetts 02454, United States*

Complete contact information is available at: https://pubs.acs.org/10.1021/acs.bioconjchem.2c00084

Notes

The authors declare no competing financial interest.

■ ACKNOWLEDGMENTS

This work is partially supported by NIH (CA142746) and NSF (DMR-2011846 and OAC1920147).

■ REFERENCES

(1) Rodriguez, H.; Zenklusen, J. C.; Staudt, L. M.; Doroshow, J. H.; Lowy, D. R. The next horizon in precision oncology: Proteogenomics to inform cancer diagnosis and treatment. *Cell* **2021**, *184*, 1661−1670.

(2) Yan, R.; Hu, Y.; Liu, F.; Wei, S.; Fang, D.; Shuhendler, A. J.; Liu, H.; Chen, H. Y.; Ye, D. Activatable NIR Fluorescence/MRI Bimodal Probes for in Vivo Imaging by Enzyme-Mediated Fluorogenic Reaction and Self-Assembly. *J. Am. Chem. Soc.* **2019**, *141*, 10331−10341.

(3) Zhang, M.; Wang, L.; Zhao, Y.; Wang, F.; Wu, J.; Liang, G. Using Bioluminescence Turn-On To Detect Cysteine in Vitro and in Vivo. *Anal. Chem.* **2018**, *90*, 4951−4954.

(4) Gao, W.; Xing, B.; Tsien, R. Y.; Rao, J. Novel fluorogenic substrates for imaging beta-lactamase gene expression. *J. Am. Chem. Soc.* **2003**, *125*, 11146−7.

(5) Wang, Z.; Xing, B. Small-molecule fluorescent probes: big future for specific bacterial labeling and infection detection. *Chem. Commun.* **2021**, *58*, 155−170.

(6) Zlokarnik, G.; Negulescu, P. A.; Knapp, T. E.; Mere, L.; Burres, N.; Feng, L.; Whitney, M.; Roemer, K.; Tsien, R. Y. Quantitation of Transcription and Clonal Selection of Single Living Cells with β-Lactamase as Reporter. *Science* **1998**, *279*, 84−88.

(7) Tamura, T.; Fujisawa, A.; Tsuchiya, M.; Shen, Y.; Nagao, K.; Kawano, S.; Tamura, Y.; Endo, T.; Umeda, M.; Hamachi, I. Organelle membrane-specific chemical labeling and dynamic imaging in living cells. *Nat. Chem. Biol.* **2020**, *16*, 1361−1367.
(8) Tan, W.; Zhang, Q.; Wang, J.; Yi, M.; He, H.; Xu, B. Enzymatic Assemblies of Thiophosphopeptides Instantly Target Golgi Apparatus and Selectively Kill Cancer Cells*. *Angew. Chem., Int. Ed.* **2021**, *60*, 12796−12801.
(9) Kulkarni-Gosavi, P.; Makhoul, C.; Gleeson, P. A. Form and function of the Golgi apparatus: scaffolds, cytoskeleton and signalling. *FEBS Lett.* **2019**, *593*, 2289−2305.
(10) Lee, M. C.; Miller, E. A.; Goldberg, J.; Orci, L.; Schekman, R. Bi-directional protein transport between the ER and Golgi. *Annu. Rev. Cell Dev. Biol.* **2004**, *20*, 87−123.
(11) Bivona, T. G.; Pérez de Castro, I.; Ahearn, I. M.; Grana, T. M.; Chiu, V. K.; Lockyer, P. J.; Cullen, P. J.; Pellicer, A.; Cox, A. D.; Philips, M. R. Phospholipase Cγ activates Ras on the Golgi apparatus by means of RasGRP1. *Nature* **2003**, *424*, 694−698.
(12) Farber-Katz, S. E.; Dippold, H. C.; Buschman, M. D.; Peterman, M. C.; Xing, M.; Noakes, C. J.; Tat, J.; Ng, M. M.; Rahajeng, J.; Cowan, D. M.; Fuchs, G. J.; Zhou, H.; Field, S. J. DNA damage triggers golgi dispersal via DNA-PK and GOLPH3. *Cell* **2014**, *156*, 413−427.
(13) Rieger, L.; O'Shea, S.; Godsmark, G.; Stanicka, J.; Kelly, G.; O'Connor, R. IGF-1 receptor activity in the Golgi of migratory cancer cells depends on adhesion-dependent phosphorylation of Tyr1250 and Tyr1251. *Sci. Signal.* **2020**, *13*, 1 DOI: 10.1126/scisignal.aba3176.
(14) Åkerfeldt, S. Hydrolysis of Cysteamine S-Phosphate. *J. Org. Chem.* **1964**, *29*, 493.
(15) Reches, M.; Gazit, E. Casting Metal Nanowires Within Discrete Self-Assembled Peptide Nanotubes. *Science* **2003**, *300*, 625−627.
(16) Gao, Y.; Shi, J.; Yuan, D.; Xu, B. Imaging enzyme-triggered self-assembly of small molecules inside live cells. *Nat. Commun.* **2012**, *3*, 1−8.
(17) Yang, Z.; Gu, H.; Fu, D.; Gao, P.; Lam, J. K.; Xu, B. Enzymatic formation of supramolecular hydrogels. *Adv. Mater.* **2004**, *16*, 1440−1444.
(18) Zhou, J.; Du, X.; Li, J.; Yamagata, N.; Xu, B. Taurine boosts cellular uptake of small D-peptides for enzyme-instructed intracellular molecular self-assembly. *J. Am. Chem. Soc.* **2015**, *137*, 10040−10043.
(19) Bonifacino, J. S.; Rojas, R. Retrograde transport from endosomes to the trans-Golgi network. *Nat. Rev. Mol. Cell Bio.* **2006**, *7*, 568−579.
(20) Lowe, M.; Gonatas, N. K.; Warren, G. The mitotic phosphorylation cycle of the cis-Golgi matrix protein GM130. *J. Cell Biol.* **2000**, *149*, 341−356.
(21) Kellokumpu, S. Golgi pH, Ion and Redox Homeostasis: How Much Do They Really Matter? *Front. Cell Dev. Biol.* **2019**, *7*, 93−93a.
(22) Paladino, S.; Lebreton, S.; Tivodar, S.; Formiggini, F.; Ossato, G.; Gratton, E.; Tramier, M.; Coppey-Moisan, M.; Zurzolo, C. Golgi sorting regulates organization and activity of GPI proteins at apical membranes. *Nat. Chem. Biol.* **2014**, *10*, 350−357.
(23) Rouillard, A. D.; Gundersen, G. W.; Fernandez, N. F.; Wang, Z.; Monteiro, C. D.; McDermott, M. G.; Ma'ayan, A. The harmonizome: a collection of processed datasets gathered to serve and mine knowledge about genes and proteins. *Database* **2016**, *2016*, baw100.
(24) Kretzschmar, M. Regulation of hepatic glutathione metabolism and its role in hepatotoxicity. *Exp. Toxicol. Pathol.* **1996**, *48*, 439−446.
(25) Lin, H.-L.; Liu, T.-Y.; Chau, G.-Y.; Lui, W.-Y.; Chi, C.-W. Comparison of 2-methoxyestradiol-induced, docetaxel-induced, and paclitaxel-induced apoptosis in hepatoma cells and its correlation with reactive oxygen species. *Cancer* **2000**, *89*, 983−994.
(26) Rosenwald, A. G.; Pagano, R. E. Inhibition of glycoprotein traffic through the secretory pathway by ceramide. *J. Biol. Chem.* **1993**, *268*, 4577−4579.
(27) Weigel, A. V.; Chang, C.-L.; Shtengel, G.; Xu, C. S.; Hoffman, D. P.; Freeman, M.; Iyer, N.; Aaron, J.; Khuon, S.; Bogovic, J.; Qiu, W.; Hess, H. F.; Lippincott-Schwartz, J. ER-to-Golgi protein delivery through an interwoven, tubular network extending from ER. *Cell* **2021**, *184*, 2412−2429.
(28) Simopoulos, T. T.; Jencks, W. P. Alkaline Phosphatase Is an Almost Perfect Enzyme. *Biochemistry* **1994**, *33*, 10375−10380.
(29) Gao, Y.; Kuang, Y.; Du, X.; Zhou, J.; Chandran, P.; Horkay, F.; Xu, B. Imaging self-assembly dependent spatial distribution of small molecules in a cellular environment. *Langmuir* **2013**, *29*, 15191−200.

https://doi.org/10.1021/acs.bioconjchem.2c00084
Bioconjugate Chem. XXXX, XXX, XXX−XXX